

# A nonlinear piezoelectric 3D-beam finite element formulation

A. Butz\*, S. Klinkel, W. Wagner

*Institut für Baustatik, Universität Karlsruhe, Kaiserstr. 12, 76131 Karlsruhe, Germany*

## Abstract

This paper presents a finite element formulation of a three-dimensional piezoelectric beam which includes geometrical and material nonlinearities. Based on the Timoshenko theory, an eccentric beam formulation is introduced which provides an efficient model of piezoelectric multilayered structures. The geometrically nonlinear assumption allows the calculation of large deformations including buckling behavior. A quadratic approximation of the electric potential through the cross section of the beam ensures the fulfilment of the charge conservation law exactly. To account for the material nonlinearities which arise in ferroelectric materials, the Preisach model is implemented in the finite element formulation.

*Keywords:* Piezoelectricity, Finite beam element; Smart material; Preisach model

## 1. Introduction

For the development of piezoelectric components, the finite element method is a well suited tool. Due to the rod like structures of many of such devices, it is reasonable to use finite beam elements for an efficient numerical simulation. In the literature different piezoelectric beam models are found, see e.g. [1], which are usually based on the linear theory. In recent years some geometrically nonlinear formulations have been published, see e.g. [2].

To model piezoelectric material nonlinearities one may follow thermodynamically motivated approaches, e.g. [3] or by using the phenomenological Preisach model, e.g. [4]. The advantage of the latter model is its simple numerical implementation and the experimental determination of the material parameters [5].

This formulation presents a finite beam element that includes both geometrical and material nonlinearities. It provides a simulation tool which is characterized by high efficiency and a wide range of applications. The essential features of the proposed model are summarized as follows:

- A three-dimensional, eccentric beam formulation using the Timoshenko kinematic is introduced.
- A geometrically nonlinear formulation is considered,

which accounts for moderate rotations and allows the investigation of buckling problems.

- A quadratic approximation of the electric potential ensures the fulfilment of the charge conservation law for bending loads.
- To take into account high electrical loads, a material nonlinear model is implemented. The additional remanent part of the polarization is determined by employing the Preisach model.

## 2. Governing equations

On the basis of linear piezoelectricity the remanent polarization  $\vec{P}^i$  is included in the constitutive equations to account for nonlinear ferroelectric behavior. The nonlinear constitutive equations read

$$\begin{aligned} \mathbf{S} &= \mathbb{C} : \mathbf{E} - \mathbf{e} \cdot \vec{E} \\ \vec{D} - \vec{P}^i &= \mathbf{e}^T : \mathbf{E} + \boldsymbol{\epsilon} \cdot \vec{E} \end{aligned} \quad (1)$$

Here,  $\mathbf{S}$ ,  $\vec{D}$ ,  $\mathbf{E}$  and  $\vec{E}$  are second Piola-Kirchhoff stresses, dielectric displacements, Green-Lagrangian strains and electric field. The material properties are defined by the elasticity matrix  $\mathbb{C}$ , the permittivity matrix  $\boldsymbol{\epsilon}$  and the piezoelectric matrix  $\mathbf{e}$  which is now a function of the electric field. The nonlinear strains  $\mathbf{E}$  and the electric field  $\vec{E}$  are functions of the displacements  $\mathbf{u} = [u, v, w]^T$  and the electric potential  $\phi$ :

\* Corresponding author. Tel.: +49 (721) 608 6893; Fax: +49 (721) 608 6015; E-mail: alexander.butz@bs.uni-karlsruhe.de

$$\mathbf{E} = \frac{1}{2}(\text{Grad } \mathbf{u} + \text{Grad } \mathbf{u}^T + \text{Grad } \mathbf{u}^T \text{Grad } \mathbf{u}) \quad (2)$$

$$\vec{\mathbf{E}} = -\text{Grad } \phi \quad (3)$$

The mechanical and electrical field equations in the reference configuration  $\mathcal{B}_0$  are described by

$$\text{Div } \mathbf{P} + \mathbf{b} = 0 \quad \text{in } \mathcal{B}_0 \quad (4)$$

$$\text{Div } \vec{\mathbf{D}} = 0 \quad \text{in } \mathcal{B}_0 \quad (5)$$

with the body forces  $\mathbf{b}$ . The first Piola-Kirchhoff stress tensor  $\mathbf{P}$  may be expressed as  $\mathbf{P} = \mathbf{F} \mathbf{S}$  where  $\mathbf{F} = \text{Grad } \mathbf{x}$  is the deformation gradient and  $\mathbf{x}$  the position vector of the current configuration. The mechanical and electrical boundary conditions are given as

$$\mathbf{S} \cdot \mathbf{n} - \vec{\mathbf{t}} = 0 \quad \text{on } \partial_t \mathcal{B}_0 \quad (6)$$

$$\vec{\mathbf{D}} \cdot \mathbf{n} - (\bar{\sigma} - \bar{\sigma}^i) = 0 \quad \text{on } \partial_\sigma \mathcal{B}_0 \quad (7)$$

in which  $\vec{\mathbf{t}}$  is defined as the traction vector on the surface  $\partial_t \mathcal{B}_0$  and  $\mathbf{n}$  as the unit normal vector,  $\bar{\sigma}$  represents the free charge density on the surface  $\partial_\sigma \mathcal{B}_0$ , and  $\bar{\sigma}^i$  corresponds to the surface charge due to  $\vec{\mathbf{P}}$ . The weak form is derived by multiplication of Eqs. (4), (5) with the test functions  $\delta \mathbf{u}$  and  $\delta \phi$ , integration over the domain  $\mathcal{B}_0$  and applying standard arguments leads to

$$\int_{\mathcal{B}_0} \mathbf{S} : \delta \mathbf{E} + \vec{\mathbf{D}} \cdot \delta \vec{\mathbf{E}} dV - \int_{\mathcal{B}_0} \mathbf{b} \cdot \delta \mathbf{u} dV - \int_{\partial_t \mathcal{B}_0} \vec{\mathbf{t}} \cdot \delta \mathbf{u} dS + \int_{\partial_\sigma \mathcal{B}_0} \vec{\mathbf{D}} \cdot \mathbf{n} \delta \phi dS = 0 \quad (8)$$

Here the operator  $dS$  represents the integration over the surface of the beam. In the geometrically nonlinear case

the weak form is solved within the finite element method by applying the Newton-Raphson scheme. For constant loading the linearization of Eq. (8) is derived as

$$\int_{\mathcal{B}_0} \delta \mathbf{E} : \mathbb{C} : \Delta \mathbf{E} dV + \int_{\mathcal{B}_0} \Delta \delta \mathbf{E} : \mathbf{S} dV + \int_0^1 \delta \vec{\mathbf{E}} \cdot \boldsymbol{\epsilon}^T : \Delta \mathbf{E} dV + \int_{\mathcal{B}_0} \delta \mathbf{E}_m : \boldsymbol{\epsilon} \cdot \Delta \vec{\mathbf{E}} dV + \int_{\mathcal{B}_0} \delta \vec{\mathbf{E}} \cdot \boldsymbol{\epsilon} \cdot \Delta \vec{\mathbf{E}} dV \quad (9)$$

In the case of material nonlinearities the quasi-Newton method is employed.

### 3. Beam formulation

The kinematic description of the beam model is based on the Timoshenko theory. The displacement vector  $\mathbf{u} = [u, v, w]^T$  is a function of the beam displacement vector  $\mathbf{v}$  and the matrix  $\mathbf{A}$  and reads

$$\mathbf{u}(x, y, z) = \mathbf{A}(y, z) \mathbf{v}(x) \quad (10)$$

$$\mathbf{A} = \begin{bmatrix} 1 & 0 & 0 & 0 & z & -y \\ 0 & 1 & 0 & -z & 0 & 0 \\ 0 & 0 & 1 & y & 0 & 0 \end{bmatrix} \quad \text{and} \quad \mathbf{v} = \begin{bmatrix} u_0 \\ v_0 \\ w_0 \\ \varphi_x \\ \varphi_y \\ \varphi_z \end{bmatrix} \quad (11)$$

$u_0, v_0, w_0$  represent the displacements and  $\varphi_x, \varphi_y, \varphi_z$  are rotations, see Fig. 1. The beam strain  $\mathbf{E}_b = [E_{11}, 2 E_{12}, 2 E_{13}]^T$  is decomposed as

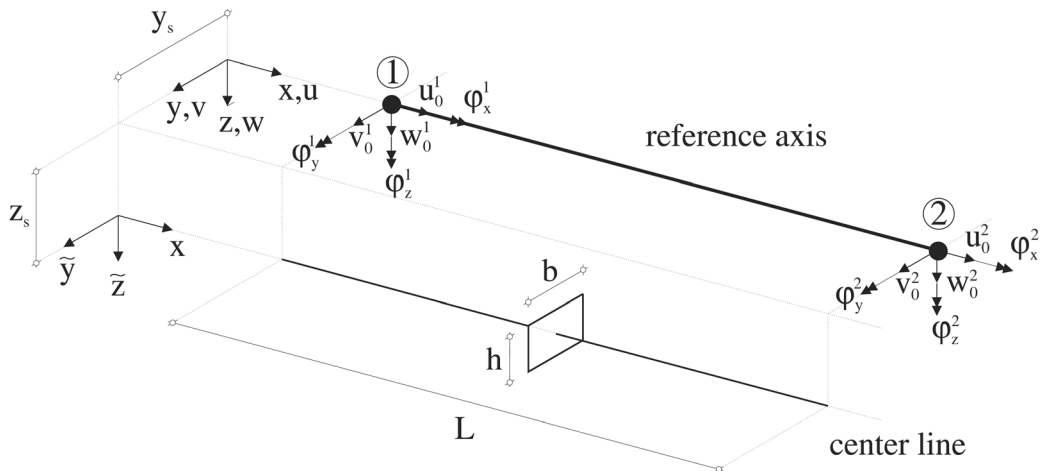


Fig. 1. Eccentric beam model.

$$\mathbf{E}_b = \mathbf{A}(y,z) \hat{\mathbf{E}}(x) \quad (12)$$

where  $\hat{\mathbf{E}}$  is defined by

$$\hat{\mathbf{E}} = \begin{bmatrix} u_{0,x} + \frac{1}{2}(v_{0,x})^2 + \frac{1}{2}(w_{0,x})^2 \\ v_{0,x} - \varphi_z \\ w_{0,x} + \varphi_y \\ \varphi_{x,x} \\ \varphi_{y,x} \\ \varphi_{z,x} \end{bmatrix} \quad (13)$$

This assumption does not consider all nonlinear parts of Eq. (2) but is sufficient to account for moderate rotations and buckling behavior.

For the electric potential the following distribution is assumed:

$$\phi(x,y,z) = \bar{\mathbf{a}}^T(y,z) \boldsymbol{\phi}(x) \quad (14)$$

with

$$\bar{\mathbf{a}}(y,z) = \begin{bmatrix} 1 \\ y \\ z \\ \left(\frac{b^2}{4} - \tilde{y}^2\right) \\ \left(\frac{b^2}{4} - \tilde{z}^2\right) \end{bmatrix} \quad \text{and} \quad \boldsymbol{\phi}(x) = \begin{bmatrix} c_1 \\ c_2 \\ c_3 \\ c_4 \\ c_5 \end{bmatrix} \quad (15)$$

The constants  $c_1$  to  $c_5$  are unknown and correspond to the electrical degrees of freedom. Using the approximations of Eq. (14) in Eq. (3), the electric field is decomposed as

$$\vec{\mathbf{E}}(x,y,z) = \bar{\mathbf{A}}(y,z) \hat{\mathbf{E}}(x) \quad (16)$$

with

$$\bar{\mathbf{A}} = - \begin{bmatrix} 0 & 0 & 0 & 0 & 0 & 1 & \tilde{y} & \tilde{z} & \left(\frac{b^2}{4} - \tilde{y}^2\right) & \left(\frac{b^2}{4} - \tilde{z}^2\right) \\ 0 & 1 & 0 & -2\tilde{y} & 0 & 0 & 0 & 0 & 0 & 0 \\ 0 & 0 & 1 & 0 & -2\tilde{z} & 0 & 0 & 0 & 0 & 0 \end{bmatrix} \quad (17)$$

and

$$\hat{\mathbf{E}} = [c_1, c_2, c_3, c_4, c_5, c_{1,x}, c_{2,x}, c_{3,x}, c_{4,x}, c_{5,x}]^T \quad (18)$$

Following common assumptions in beam theory, the stress state is reduced to  $\mathbf{S}_b = [S_{11}, S_{12}, S_{13}]^T$  whereas  $\mathbf{S}_c = [S_{22}, S_{33}, S_{23}]^T = \mathbf{0}$  is assumed. Partitioning Eq. (1) by consideration of  $\mathbf{E}_b = [E_{11}, 2 E_{12}, 2 E_{13}]^T$  and  $\mathbf{E}_c = [E_{22}, E_{33}, 2 E_{23}]^T$  results in

$$\begin{bmatrix} \mathbf{S}_b \\ \mathbf{S}_c \\ \vec{\mathbf{D}} - \vec{\mathbf{P}}^i \end{bmatrix} = \begin{bmatrix} \mathbb{C}_b & \mathbb{C}_{bc} & -\mathbf{e}_b \\ \mathbb{C}_{bc}^T & \mathbb{C}_c & -\mathbf{e}_c \\ \mathbf{e}_b^T & \mathbf{e}_c^T & \boldsymbol{\epsilon} \end{bmatrix} \begin{bmatrix} \mathbf{E}_b \\ \mathbf{E}_c \\ \vec{\mathbf{E}} \end{bmatrix} \quad (19)$$

and leads to the condensed material matrices  $\tilde{\mathbb{C}}$ ,  $\tilde{\mathbf{e}}$  and  $\tilde{\boldsymbol{\epsilon}}$ , which are derived as

$$\begin{aligned} \tilde{\mathbb{C}} &= \mathbb{C}_b - \mathbb{C}_{bc} \mathbb{C}_c^{-1} \mathbb{C}_{bc}^T & \tilde{\mathbf{e}} &= \mathbf{e}_b - \mathbb{C}_{bc} \mathbb{C}_c^{-1} \mathbf{e}_c \\ \tilde{\boldsymbol{\epsilon}} &= \boldsymbol{\epsilon} + \mathbf{e}_c^T \mathbb{C}_c^{-1} \mathbf{e}_c \end{aligned} \quad (20)$$

The weak form of the beam formulation is obtained by substituting the material matrices Eq. (20) and  $\mathbf{E}_b$  into Eq. (8). This holds analogously for the linearized weak form, Eq. (9).

#### 4. Material nonlinear model

The implemented material model is restricted to ferroelectric nonlinearities. Nonlinear effects caused by high stresses are not considered. The ferroelectric hysteresis is approximated by using the Preisach model, see e.g. [5]. The basic idea of the Preisach model states that a hysteresis loop is composed by the superposition of different simple elementary hysteresis operators, see Fig. 2. It is defined by the up- and down-switching values  $\alpha$  and  $\beta$  and the output value  $\hat{\gamma}_{\alpha\beta}(u)$  that is  $+1$  or  $-1$  and depends on the input value  $u$ . The global output value  $f(u(t))$  is expressed as an integral over the output of all elementary operators

$$f(u(t)) = \int_{\alpha > \beta} \mu(\alpha, \beta) \hat{\gamma}_{\alpha\beta}(u(t)) d\alpha d\beta \quad (21)$$

The expression  $\mu(\alpha, \beta)$  is called the Preisach function

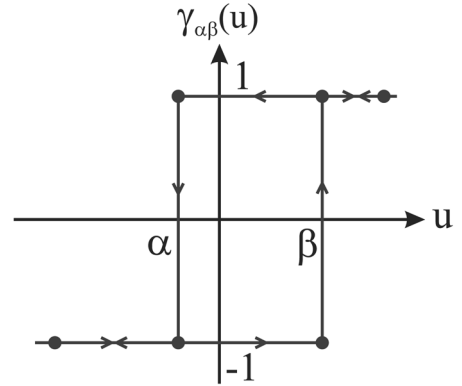


Fig. 2. Elementary hysteresis operator.

and describes the distribution of the elementary hysteresis operators. In the presented formulation,  $\vec{\mathbf{E}}_z$  represents the input value and  $\vec{\mathbf{P}}_z^i$  the output value. After the evaluation of the remanent polarization, the piezoelectric matrix  $\tilde{\boldsymbol{\epsilon}}$  is updated with respect to the current value of  $\vec{\mathbf{P}}_z^i$ . Therefore  $\tilde{\boldsymbol{\epsilon}}$  is multiplied by the normalized polarization  $\vec{\mathbf{P}}_z^i / P_{sat}$  with  $P_{sat}$  as saturation polarization. A detailed description of the Preisach model may be found in [5].

## 5. Finite element approximation

The displacements and the electric potential are approximated with linear shape functions  $N_I$ . This leads to a two node finite beam element with six mechanical degrees of freedom  $\mathbf{v}_I = [u_0, v_0, w_0, \varphi_x, \varphi_y, \varphi_z]^T$  and five electrical degrees of freedom  $\phi_I = [c_1, c_2, c_3, c_4, c_5]^T$  for each node  $I$ . The interpolation of the displacements, the electric potential, their derivatives, virtual and linearized quantities are approximated as follows:

$$\begin{aligned} \mathbf{u}^h &= \mathbf{A} \mathbf{N} \mathbf{v}, & \delta \mathbf{u}^h &= \mathbf{A} \mathbf{N} \delta \mathbf{v}, & \Delta \mathbf{u}^h &= \mathbf{A} \mathbf{N} \Delta \mathbf{v}, \\ \mathbf{u}_{,x}^h &= \mathbf{A} \mathbf{N}_{,x} \mathbf{v} \end{aligned} \quad (22)$$

$$\phi^h = \bar{\mathbf{a}} \bar{\mathbf{N}} \phi \quad \delta \phi^h = \bar{\mathbf{a}} \bar{\mathbf{N}} \delta \phi, \quad \Delta \phi^h = \bar{\mathbf{a}} \bar{\mathbf{N}} \Delta \phi,$$

$$\phi_{,x}^h = \bar{\mathbf{a}} \bar{\mathbf{N}}_{,x} \phi$$

with the vectors  $\mathbf{v}^T = [v_1^T, v_2^T]$  and  $\phi^T = [\phi_1^T, \phi_2^T]$ . The matrices  $\mathbf{N}$  and  $\bar{\mathbf{N}}$  are given as

$$\begin{aligned} \mathbf{N} &= [\mathbf{N}_1, \mathbf{N}_2], & \bar{\mathbf{N}} &= [\bar{\mathbf{N}}_1, \bar{\mathbf{N}}_2], & \text{with } N_I &= N_I \mathbf{1}_{6 \times 6}, \\ \bar{N}_I &= N_I \mathbf{1}_{5 \times 5} \end{aligned} \quad (23)$$

where  $N_1 = 1 - \frac{x}{L}$  and  $N_2 = \frac{x}{L}$ . With respect to Eqs. (12), (13), (16) and (18) the approximations of the beam strains and of the electric field are derived as

$$\begin{aligned} \delta \mathbf{E}_b^h &= \mathbf{A} \mathbf{B} \delta \mathbf{v} & \Delta \mathbf{E}_b^h &= \mathbf{A} \mathbf{B} \Delta \mathbf{v} \\ \delta \bar{\mathbf{E}}^h &= \bar{\mathbf{A}} \bar{\mathbf{B}} \delta \phi & \Delta \bar{\mathbf{E}}^h &= \bar{\mathbf{A}} \bar{\mathbf{B}} \Delta \phi \end{aligned} \quad (24)$$

with  $\mathbf{B} = [\mathbf{B}_1, \mathbf{B}_2]$  and  $\bar{\mathbf{B}} = [\bar{\mathbf{B}}_1, \bar{\mathbf{B}}_2]$ . The matrices  $\mathbf{B}_I$  and  $\bar{\mathbf{B}}_I$  are determined as

$$\begin{aligned} \mathbf{B}_I &= \begin{bmatrix} N_{I,x} & v_{0,x} N_{I,x} & w_{0,x} N_{I,x} & 0 & 0 & 0 \\ 0 & N_{I,x} & 0 & 0 & 0 & -N_I \\ 0 & 0 & N_{I,x} & 0 & N_I & 0 \\ 0 & 0 & 0 & N_{I,x} & 0 & 0 \\ 0 & 0 & 0 & 0 & N_{I,x} & 0 \\ 0 & 0 & 0 & 0 & 0 & N_{I,x} \end{bmatrix} \\ \bar{\mathbf{B}}_I &= \begin{bmatrix} N_I & 0 & 0 & 0 & 0 \\ 0 & N_I & 0 & 0 & 0 \\ 0 & 0 & N_I & 0 & 0 \\ 0 & 0 & 0 & N_I & 0 \\ 0 & 0 & 0 & 0 & N_I \\ N_{I,x} & 0 & 0 & 0 & 0 \\ 0 & N_{I,x} & 0 & 0 & 0 \\ 0 & 0 & N_{I,x} & 0 & 0 \\ 0 & 0 & 0 & N_{I,x} & 0 \\ 0 & 0 & 0 & 0 & N_{I,x} \end{bmatrix} \end{aligned} \quad (25)$$

Considering Eqs. (22), (24) in (8) and (9), the approximation of the weak form and its linearization on element level reads

$$\mathbf{G}^e = \begin{bmatrix} \delta \mathbf{v} \\ \delta \phi \end{bmatrix}^T \left( \underbrace{\begin{bmatrix} \mathbf{K}_{vv}^e & -\mathbf{K}_{v\phi}^e \\ \mathbf{K}_{\phi v}^e & \mathbf{K}_{\phi\phi}^e \end{bmatrix}}_{\mathbf{K}^e} \underbrace{\begin{bmatrix} \Delta \mathbf{v} \\ \Delta \phi \end{bmatrix}}_{\Delta \mathbf{d}} - \underbrace{\begin{bmatrix} \mathbf{F}^e \\ -\mathbf{Q}^e \end{bmatrix}}_{\mathbf{R}^e} \right) \quad (26)$$

with

$$\mathbf{K}_{vv}^e = \int_{L^e} \mathbf{B}^T \left( \int_{A^e} \mathbf{A}^T \tilde{\mathbf{c}} \mathbf{A} dA \right) \mathbf{B} ds + \mathbf{G}^e \quad (27)$$

$$\mathbf{K}_{v\phi}^e = \int_{L^e} \mathbf{B}^T \left( \int_{A^e} \mathbf{A}^T \tilde{\mathbf{e}} \bar{\mathbf{A}} dA \right) \bar{\mathbf{B}} ds = \mathbf{K}_{\phi v}^e \quad (28)$$

$$\mathbf{K}_{\phi\phi}^e = \int_{L^e} \bar{\mathbf{B}}^T \left( \int_{A^e} \bar{\mathbf{A}}^T \tilde{\mathbf{e}} \bar{\mathbf{A}} dA \right) \bar{\mathbf{B}} ds \quad (29)$$

Here  $dA$  describes the integration through the cross section and  $ds$  the integration along the beam axis. In Eq. (26)  $\mathbf{K}^e$  denotes the tangent stiffness matrix and  $\mathbf{R}^e$  is the load vector. The expression  $\mathbf{G}^e$  represents the initial stress stiffness matrix and is given as

$$\mathbf{G}^e = \begin{bmatrix} \mathbf{G}_{11} & \mathbf{G}_{12} \\ \mathbf{G}_{21} & \mathbf{G}_{22} \end{bmatrix} \text{ with } \mathbf{G}_{IK} = \begin{bmatrix} 0 & 0 & 0 & 0 & 0 & 0 \\ 0 & G_{IK} & 0 & 0 & 0 & 0 \\ 0 & 0 & G_{IK} & 0 & 0 & 0 \\ 0 & 0 & 0 & 0 & 0 & 0 \\ 0 & 0 & 0 & 0 & 0 & 0 \\ 0 & 0 & 0 & 0 & 0 & 0 \end{bmatrix} \quad (30)$$

and

$$G_{IK} = \int_{L^e} N_{I,x} \left( \int_{A^e} S_{11} dA \right) N_{K,x} ds \quad (31)$$

The mechanical load vector  $\mathbf{F}^e$  and the charge vector  $\mathbf{Q}^e$  are defined as

$$\begin{aligned} \mathbf{F}_I^e &= \int_{\partial L^e} \mathbf{N}^T \mathbf{A}^T \bar{\mathbf{t}} dS + \int_{L^e} \mathbf{N}^T \left( \int_{A^e} \mathbf{A}^T \mathbf{b} dA \right) ds - \\ & \int_{L^e} \mathbf{B}^T \left( \int_{A^e} \mathbf{A}^T \mathbf{S}_b dA \right) ds \end{aligned}$$

$$\mathbf{Q}_I^e = \int_{\partial L^e} (\bar{\sigma} - \bar{\sigma}^i) N_I \bar{\mathbf{a}} dS + \int_{L^e} \bar{\mathbf{B}}^T \left( \int_{A^e} \bar{\mathbf{A}}^T \bar{\mathbf{P}}^i dA \right) ds \quad (32)$$

After assembly over all elements  $\mathbf{K}_T = A_{e=1}^{\text{nelm}} \mathbf{K}^e$ ,  $\mathbf{R} = A_{e=1}^{\text{nelm}} \mathbf{R}^e$  and  $\Delta \mathbf{D} = A_{e=1}^{\text{nelm}} \Delta \mathbf{d}^e$  one obtains the following global equation;

$$\mathbf{K}_T \Delta \mathbf{D} - \mathbf{R} = \mathbf{0} \quad (33)$$

## 6. Numerical examples

### 6.1. Simple test for hysteresis loops

To verify the implemented material nonlinearities, this example considers a piezoelectric cantilever, see Fig. 3. It consists of barium titanate ceramic material that is polarized in  $z$ -direction. With respect to [6], the material parameters are given as

$$\begin{aligned} C_{11} &= 166 \text{ GPa} & C_{33} &= 162 \text{ GPa} & C_{44} &= 42.9 \text{ GPa} \\ C_{66} &= 44.8 \text{ GPa} & C_{12} &= 76.6 \text{ GPa} & C_{13} &= 77.5 \text{ GPa} \\ e_{31} &= -4.4 \text{ C/m}^2 & e_{33} &= 18.6 \text{ C/m}^2 & e_{15} &= 11.6 \text{ C/m}^2 \\ \epsilon_{11} &= 1.12 \cdot 10^{-8} \frac{\text{C}}{\text{Vm}} & \epsilon_{22} &= 1.12 \cdot 10^{-8} \frac{\text{C}}{\text{Vm}} \\ \epsilon_{33} &= 1.26 \cdot 10^{-8} \frac{\text{C}}{\text{Vm}} \end{aligned} \quad (34)$$

The coercive field strength is assumed as  $E_c = 1000$  [V/mm] and the saturation polarization as  $P_{\text{sat}} = 0.26$  [C/m<sup>2</sup>]. An electric field  $\bar{E}_z(t) = 2000 \cdot \sin(t)$  [V/mm] as a function of time  $t$  is applied. The Preisach function is assumed as

$$\mu(\alpha, \beta) = \frac{50}{\pi} e^{(-25(\alpha+\beta)^2 - 25(\beta-\alpha+1)^2)} \quad (35)$$

The cantilever is modelled with one finite element, see Fig. 3. Fig. 4(a) shows the typical dielectric hysteresis that appears in piezoelectric materials. The dotted line represents the irreversible part of the polarization  $\bar{P}_z^i$ . The continuous line shows the dielectric displacements

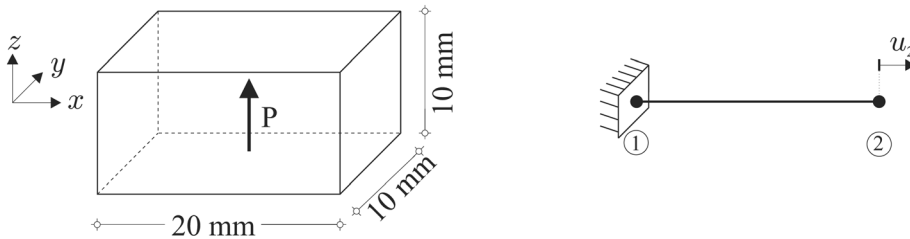


Fig. 3. Geometry and finite element model.

$\bar{D}_z$ . It consists of an irreversible part that is caused by  $\bar{P}_z^i$  and an additional reversible part from linear piezoelectricity. In Fig. 4(b) the displacement  $u_2$  is plotted versus the electric field. The result is a typical butterfly hysteresis curve that is commonly found in literature.

### 6.2. Clamped bimorph beam

In the second example a cantilever beam that consists of an aluminium and a barium titanate layer is analyzed. The geometry data are given in Fig. 5. The barium titanate is polarized in the  $z$ -direction, and the material parameters are taken from the previous example. For the aluminium layer  $E = 70.3$  GPa and  $\nu = 0.345$  are assumed. The barium titanate layer is loaded with an electric field  $\bar{E}_z$  that is increased from zero to 1000 [V/mm]. For the finite element calculation the beam is discretized with 20 elements. In Fig. 5, the tip displacement in the  $z$ -direction is plotted versus the electric field for the case of material linear and nonlinear behavior. Both calculations lead to the same deflection  $w_{Tip}$  if  $\bar{E}_z$  is much smaller than  $\bar{E}_c$ . At higher loading, the material nonlinear model accounts for domain switching effects. The reorientation of the domains leads to significant differences in the load deflection curves.

## 7. Conclusion

A finite element formulation for a piezoelectric beam model is introduced that considers geometrical or material nonlinearities. The numerical examples demonstrate the applicability for material nonlinear behavior and for layered beam structures.

## Acknowledgment

This work was supported by the Research Training Group 786 'Mixed Fields and Nonlinear Interactions' of the Deutsche Forschungsgemeinschaft (<http://www.gkmf.uni-karlsruhe.de>).

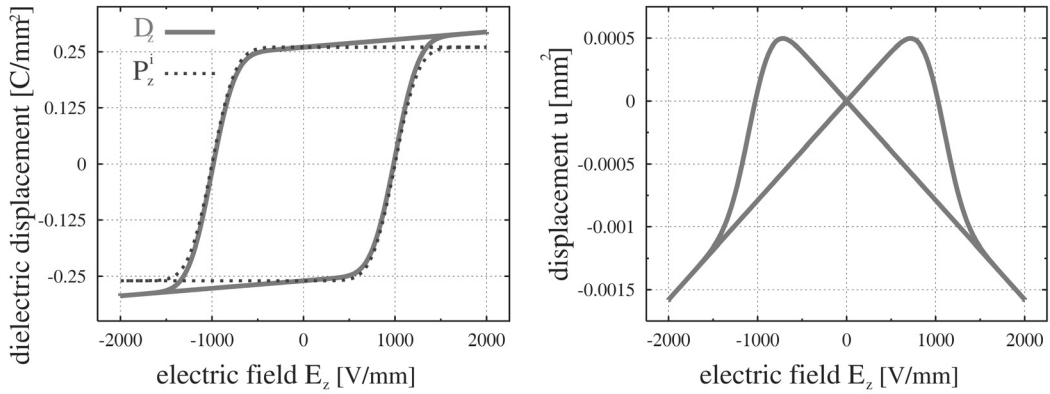


Fig. 4. Hysteresis curves.

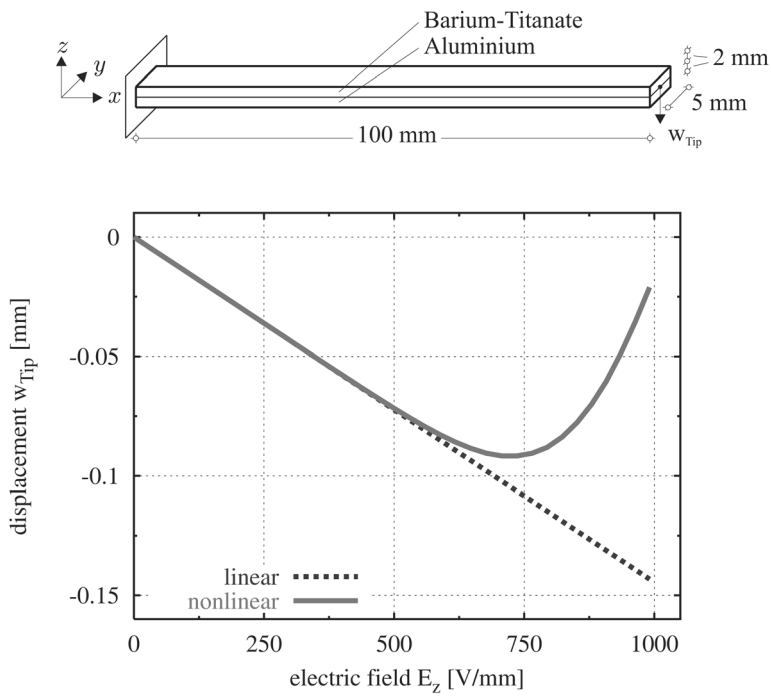


Fig. 5. Geometry of the cantilever and load deflection curve.

## References

- [1] Benjeddou A. Advances in piezoelectric finite element modeling of adaptive structural elements: a survey. *Comput Struct* 2000;76:347–363.
- [2] Mukherjee M, Chaudhuri AS. Piezolaminated beams with large deformations. *Int J Solids Struct* 2002;39:4567–4582.
- [3] Kamlah M. Ferroelectric and ferroelastic piezoceramics – modeling of electromechanical hysteresis phenomena. *Continuum Mech Thermodyn* 2001;13:219–268.
- [4] Yu Y, Naganathan N, Dukkupati R. Preisach modeling of hysteresis for piezoceramic actuator system. *Mech Mach Theory* 2002;37:49–59.
- [5] Mayergoyz ID. *Mathematical models of hysteresis and their applications*. Amsterdam, Boston, MA: Elsevier, 2003.
- [6] Jaffe B, Cook WR, Jaffe H. *Piezoelectric ceramics*. London, New York: Academic Press, 1971.